INTEGRATING POLARIMETRIC SYNTHETIC APERTURE RADAR AND IMAGING SPECTROMETRY FOR WILDLAND FUEL MAPPING IN SOUTHERN CALIFORNIA

Philip E. Dennison
Department of Geography, University of California, Santa Barbara, CA 93106
Phone: (805) 893-4519
E-mail: dennison@geog.ucsb.edu

Dar A. Roberts
Department of Geography, University of California, Santa Barbara, CA 93106
Phone: (805) 893-2276
E-mail: dar@geog.ucsb.edu

Ernest Reith
Department of Geography, University of California, Santa Barbara, CA 93106
Phone: (805) 893-4519
E-mail: ernest@geog.ucsb.edu

Jon C. Regelbrugge
Pacific Southwest Research Station, USDA Forest Service, 4955 Canyon Crest Dr., Riverside, CA 92507
Phone: (909) 680-1542
E-mail: Regelbrugge_Jon/psw_rfl@fs.fed.us

Susan L. Ustin
Department of Land, Air, and Water Resources, University of California, Davis, CA 95616
Phone: (530) 752-0621
E-mail: slustin@ucdavis.edu

ABSTRACT

Polarimetric synthetic aperture radar (SAR) and imaging spectrometry exemplify advanced technologies for mapping wildland fuels in chaparral ecosystems. In this study, we explore the potential of integrating polarimetric SAR and imaging spectrometry for mapping wildland fuels. P-band SAR and ratios containing P-band polarizations are sensitive to variations in stand age and vegetation cover for an area of chaparral in the Santa Monica Mountains of Southern California. Mean P-HV/C-HV, averaged by stand age using a GIS fire history, is shown to increase with stand age. Vegetation cover maps produced from the Advanced Visible/Near Infrared Imaging Spectrometer (AVIRIS) using Multiple Endmember Spectral Mixture Analysis (MESMA) are compared with average P-HV/C-HV for hard chaparral, soft chaparral, and grassland cover types. Mean P-HV/C-HV is demonstrated to be higher for hard chaparral than for soft chaparral and grassland. Stratifying mean ratio-stand age classes by vegetation type reveals that the ratio-stand age relationship is strongest for hard chaparral and weaker for soft chaparral and grassland. Problems with speckle, a characteristic inherent to SAR, will need to be overcome before direct fine-scale mapping of stand age and biomass in chaparral ecosystems can occur.

BACKGROUND

Fire behavior model implementations have traditionally neglected local variations in fuel properties in favor of broad fuel classes. This tendency is of particular concern in California chaparral, which demonstrates high variability in its spatial distribution of fuels. Optical remote sensing techniques have demonstrated some ability to spatially characterize chaparral fuels, providing vegetation cover, expressed liquid water, and spatial distribution of non-photosynthetic vegetation (Consentino *et al.* 1981, Franklin *et al.* 1995, Roberts *et al.* 1997, Roberts *et al.* 1998). Optical remote sensing is limited in its ability to reveal chaparral characteristics by canopy absorption and reflectance. Since vegetation response at optical wavelengths is confined to the canopy level for many canopy architectures, fuel characteristics such as biomass and live woody fuel moisture must be obtained through

other means. Active microwave sensors, specifically polarimetric SAR, have potential for complementing optically measured characteristics of chaparral fuels.

The scale of surface roughness in relation to the radar wavelength and the dielectric properties of the surface will determine the surface's backscattering properties. An example of scale effects on radar backscatter can be seen in difference between grassland and shrubland radar returns (Figure 1). The structure of grasslands is rough at C-band scale (0.056 m), allowing grasslands to strongly scatter C-band radar. Grasses lack larger structures or sufficient depth to scatter longer wavelength P-band (0.68 m) radar. Shrubs are efficient scatterers at both scales. Leaves scatter C-band radar while woody stems and increased biomass permit scattering at longer wavelengths. Given similar scales, increasing the amount of biomass available for interaction with the radar pulse will increase backscatter. Differences in backscatter for longer wavelength radar can then be linked to known biomass. Radar polarization can enhance biomass measurement; cross-polarized (HV) returns, indicative of volume scattering, are especially suited to biomass detection because of the volume scattering properties of vegetation canopies. Ratios of cross-polarized (HV) returns were found to be better than single band measures of biomass for Maine pine forest (Ranson and Guoqing, 1994). Saturation of the biomass signature and SAR speckle (caused by constructive and destructive interference of successive radar pulses) limit the sensitivity of radar biomass mapping.

Most previous work on using SAR to measure biomass has focused on temperate and tropical rain forest. Extensive work has been done on Loblolly Pine stands at the Duke Experimental Forest in North Carolina. A relationship between biomass and radar return strength has been found using ERS-1 (C-band SAR) (Kasischke *et al.*, 1994; Wang *et al.*, 1994), SIR-C (polarimetric C- and L-band SAR) (Harrell *et al.*, 1997), and AIRSAR (polarimetric C-, L-, and P-band SAR) (Kasischke *et al.*, 1995; Wang *et al.*, 1995). Similar correlations have been found for northern forests using SIR-C (Dobson *et al.*, 1995) and AIRSAR (Ranson and Guoqing, 1994). Biomass detection using SIR-C and JERS-1 (L-band SAR) has been less successful in tropical rain forest (Foody *et al.*, 1997; Luckman *et al.*, 1997; Luckman *et al.*, 1998) due to saturation of the biomass signature. The quantity of biomass necessary to achieve saturation is dependent on the radar wavelength. Short wavelength C-band will saturate at much lower biomass than longer wavelength P-band. Estimates of saturation biomass range widely for each

a)

b)

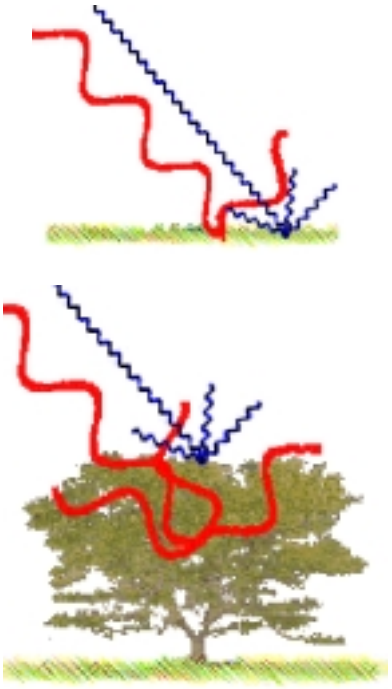

Figure 1. Radar interaction with (a) grass and (b) a shrub. C-band radar is represented in blue and P-band radar is represented in red.

frequency. Reliable saturation biomass estimates range from 0.5-2 kgm^{-2} for C-band, from 3-6 kgm^{-2} for L-band, and from 10-14 kgm^{-2} for P-band SAR (Wang *et al.*, 1994; Imhoff, 1995; Wang *et al.*, 1995; Luckman *et al.*, 1997; Luckman *et al.*, 1998). Measured chaparral biomass ranges from less than 1 kgm^{-2} for young soft chaparral to 12 kgm^{-2} for dense, mature stands of *Ceanothus* hard chaparral (Specht, 1969; DeBano and Conrad, 1978; Schlesinger and Gill, 1980; Gray, 1982; Riggan *et al.*, 1988; Regelbrugge and Conard, 1996), falling well within the limits of P-band saturation biomass.

Data Processing

Three AIRSAR full-polarimetric (C- ,L- , and P-band) flightlines over the Santa Monica Mountains were requested for the 1998 flight season. The instrument, carried aboard a NASA DC-8, was flown over the Santa Monica Mountains on April 28, 1998. Over a period of two years prior to the flight chaparral was destructively harvested at thirteen sites in the Santa Monica Mountains. Due to airspace restrictions, however, only half of the range was flown and as a result all but two of these biomass harvest sites were missed. A portion

of one image strip was selected for this study because of its central location and lack of urban features (Figure 2). Slant range images were corrected for geometry and backscatter using a 10m USGS DEM and the aircraft GPS position.

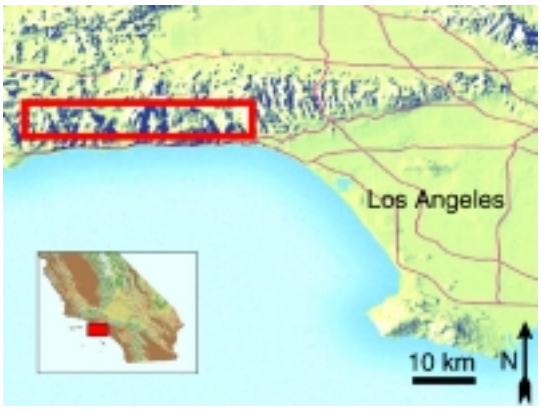

Figure 2. Study area in the Santa Monica Mountains of Southern California.

The DEM and GPS positions were used to construct an artificial radar image, and the slant range image was then registered to the artificial image. The registered radar image was corrected for terrain effects using local incidence angle and terrain calibration factor calculated from the DEM, as described in Albright *et al.*, 1998. The terrain calibration factor is used to correct backscatter for variations in local incidence angle. It is described in van Zyl *et al.*, 1993, as:

$$\sigma^0 = \sigma * (\sin \theta_i / \sin \theta_c)$$

where σ is the backscatter cross-section, θ_c is the level ground incidence angle, and θ_i is the incidence angle. The image was further corrected by normalizing backscatter using $\cos^n\theta_i$, where n is selected such that a line fit to $\cos^n\theta_i$ versus backscatter will have a slope close to zero. This correction works well in areas with surfaces possessing similar backscattering processes, but breaks down in the urban-wildland interface, where bright double-bounce backscatterers are mixed with darker single-scattering vegetation. For future processing it may be advantageous to mask urban areas using a binary decision tree before the scene is processed. After the image set is terrain corrected, it is projected to ground range by reversing the ground-to-slant projection used to create the synthetic radar scene.

RESULTS

Corrected C-band backscatter showed little detail in HH, VV, and HV polarizations. L-band backscatter showed more detail, especially in the HV polarization, but most of the detail in vegetated areas was found in the P-band images. A ratio image was created by subtracting C-HV from P-HV in decibel space. Several fire scars were apparent in the P-HV/C-HV image. Overlaying a fire history provided by the Santa Monica Mountains National Recreation Area on the P-HV/C-HV image shows a high visual correlation with stand age (Figure 3). Especially prominent are fire scars from the 1996 Calabasas Fire (a), the 1993 Topanga Fire (b), and the 1978 Mandeville Fire (c). Using the fire history polygons, mean P-HV/C-HV was calculated for each of the stand age classes (Figure 4). P-HV/C-HV increases with stand age until approximately 25 years, after which little further increase is visible. A log curve fit to the trend possesses a r^2 of 0.66.

P-HV/C-HV was also stratified by vegetation type using a 1994 MESMA vegetation map (Gardner, 1997). Vegetation species were classified into four categories: hard chaparral, soft chaparral, grassland, and other. Mean P-HV/C-HV was then calculated for each vegetation type. Mean P-HV/C-HV is lowest for grasslands and highest for hard chaparral (Figure 5). Using the MESMA vegetation map, mean P-HV/C-HV was stratified by vegetation type. Stand age/vegetation classes with fewer than 100 members were excluded due to low sample size. The relationship between stand age and P-HV/C-HV is strongest for hard chaparral and weaker for soft chaparral and grassland (Figure 6). Log curves fit to the trends for each vegetation type produce a 0.72 r^2 for hard chaparral, a 0.62 r^2 for soft chaparral, and a 0.41 r^2 for grasslands. Since grasslands and soft chaparral will rapidly mature after a fire, adding little additional biomass, a weaker relationship between P-HV/C-HV and stand age was expected for these two vegetation types. The four-year time difference between the MESMA vegetation map and the SAR image likely decreased the statistical accuracy of the ratio-stand age fits, because the 1996 Calabasas fire converted higher biomass hard chaparral and soft chaparral areas into lower biomass hard chaparral, soft chaparral, and grasslands.

DISCUSSION

Mean P-HV/C-HV exhibits a strong correlation with stand age, but this correlation can not be used to map stand age due to radar speckle. Error bars of one standard deviation placed on the plot of stand age versus P-HV/C-HV (Figure 7) demonstrate that variation in P-HV/C-HV is too high to allow accurate mapping directly from the ratio. A median filter applied to the original band images and resampling to a lower resolution may be used to decrease the variance in P-HV/

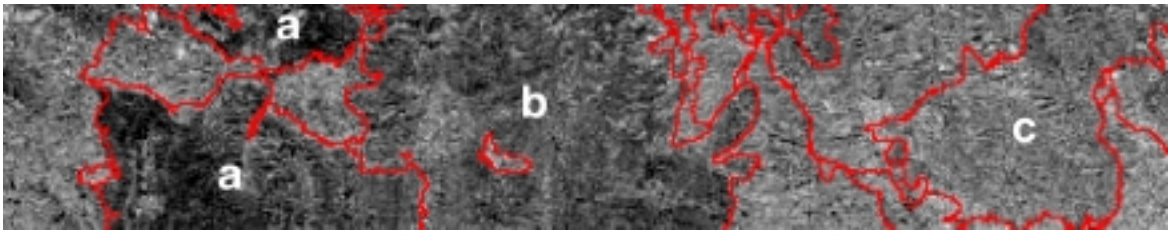

Figure 3. Fire scars are evident in the P-HV/C-HV image. Fire history polygons are outlined in red. a) The 1996 Calabasas Fire. b) The 1993 Topanga Fire. c) The 1978 Mandeville Fire.

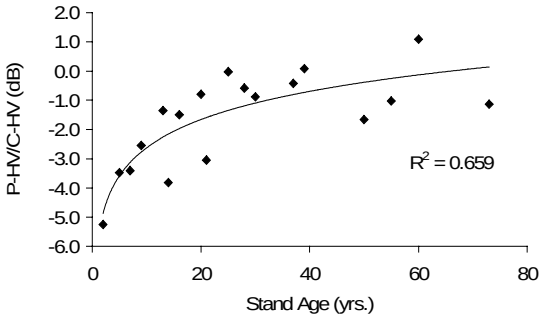

Figure 4. Stand age versus P-HV/C-HV demonstrates a strong positive trend in the first 25 years after a fire, followed by a period of little change in the ratio.

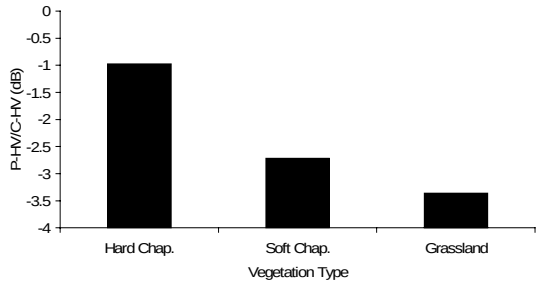

Figure 5. Hard chaparral possesses a high mean P-HV/C-HV, while soft chaparral and grassland, vegetation types with lower biomass, possess low mean P-HV/C-HV.

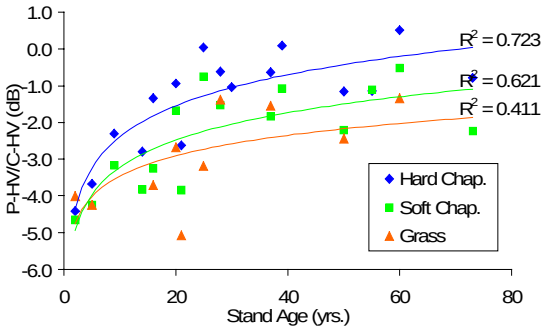

Figure 6. Stand age versus P-HV/C-HV, stratified by vegetation type. Hard chaparral exhibits the strongest relationship between stand age and the ratio.

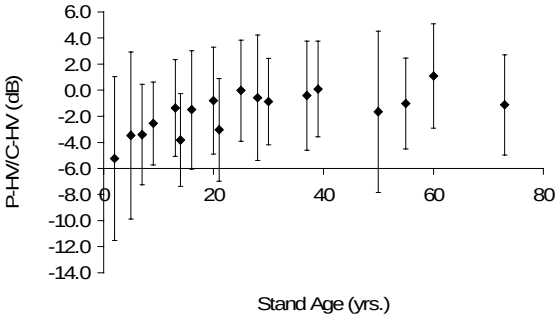

Figure 7. Stand age versus P-HV/C-HV, with error bars representing one standard deviation.

C-HV. The acquisition of a more complete data set will allow a direct relationship between biomass and P-HV/C-HV to be derived. This relationship can then be tested with further biomass sampling. Due to the specialized nature of the backscatter correction, it is unknown how P-HV/C-HV will vary between images. Masking of urban areas will probably be necessary to allow a more consistent terrain correction between images.

P-HV/C-HV did not increase with stand age after approximately 25 years age. Biomass saturation is a possible explanation, but seems unlikely given expected saturation levels of 10-14 kgm^{-2}. Speckle may overwhelm any small increase in P-HV/C-HV with stand ages over 25 years. Median filtering and aggregation to a coarser resolution will reveal whether this is the case. More likely, stand age becomes less important than site quality factors for determining hard chaparral biomass after 25 years age. Studies have found little relationship between stand age and aboveground biomass (Regelbrugge and Conard, 1996) and between stand age and dead fuel fraction (Paysen and Cohen, 1990) for chamise chaparral (*Adenostoma fasciculatum)*. P-HV/C-HV and similar SAR measures of chaparral biomass will be compared to site quality indices in future research.

CONCLUSIONS

There is a strong relationship between mean P-HV/C-HV and stand age for the study area. This relationship is improved for hard chaparral when mean P-HV/C-HV is segmented by vegetation type. Soft chaparral and grasslands show a weaker relationship between mean P-HV/C-HV and stand age. For biomass mapping to be realized, problems with speckle must be resolved and a direct relationship between biomass and P-HV/C-HV must be derived.

WORKS CITED

Albright, T. P. *et al.* (1998). "Classification of surface types using SIR-C/X-SAR, Mount Everest, Tibet." *Journal of Geophysical Research* 103(E11): 25823-37.

Consentino, M. J., Woodcock, C. E. and Franklin, J. 1981. Scene analysis for wildland fire-fuel characteristics in a mediterranean climate. *Proceedings of the fifteenth International Symposium on Remote Sensing of Environment*, 11-15 May 1981, Ann Arbor, Mich: 635-643.

DeBano, L. F. and Conrad, C. E. 1978. The effect of fire on nutrients in a chaparral ecosystem. *Ecology*, 59(3): 489-497.

Dobson, C. M. *et al.* 1995. Estimation of forest biophysical characteristics in Northern Michigan with SIR-C/X-SAR. *IEEE Transactions on Geoscience and Remote Sensing*, 33(4): 877-95.

Foody, G. M. *et al.* 1997. Observations on the relationship between SIR-C radar backscatter and the biomass of regenerating tropical forests. *International Journal of Remote Sensing*: 687-694.

Franklin, J., Swenson, J. and Shaari, D. 1995. *Forest Service Southern California Mapping Project, Santa Monica Mountains National Recreation Area, Project Description and Results*, San Diego State University, San Diego.

Gardner, M. 1997. *Mapping chaparral with AVIRIS using advanced remote sensing techniques.* Master's Thesis, University of California Santa Barbara Department of Geography.

Gray, J. T. 1982. Community structure and productivity in Ceanothus chaparral and coastal sage scrub of Southern California. *Ecological Monographs*, 52(4): 415-35.

Harrell, P. A., Kasischke, E. S., Bourgeau-Chavez, L. L., Haney, E. M. and Christensen, N. L., Jr. 1997. Evaluation of approaches to estimating aboveground biomass in southern pine forests using SIR-C data. *Remote Sensing of Environment*, 59(2): 223-233.

Imhoff, M. L. 1995. Radar backscatter and biomass saturation: ramifications for global biomass inventory. *IEEE Transactions on Geoscience and Remote Sensing*, 33(2): 511-18.

Kasischke, E. S., Bourgeau-Chavez, L. L., Christensen, N. L., Jr. and Haney, E. 1994. Observations on the sensitivity of ERS-1 SAR image intensity to changes in aboveground biomass in young loblolly pine forests. *International Journal of Remote Sensing*: 3-16.

Kasischke, E. S., Christensen, N. L., Jr. and Bourgeau-Chavez, L. L. 1995. Correlating radar backscatter with components of biomass in loblolly pine forests. *IEEE Transactions on Geoscience and Remote Sensing*, 33(3): 643-59.

Luckman, A., Baker, J., Honzak, M. and Lucas, R. 1998. Tropical forest biomass density estimation using JERS-1 SAR: Seasonal variation, confidence limits, and application to image mosaics. *Remote Sensing of Environment*: 126-139.

Luckman, A., Baker, J., Kuplich, T. M., Yanasse, C. D. C. F. and Frery, A. C. 1997. A study of the relationship between radar backscatter and regenerating tropical forest biomass for spaceborne SAR instruments. *Remote Sensing of Environment*: 1-13.

Paysen, T. E. and Cohen, J. D. 1990. Chamise chaparral dead fuel fraction is not reliably predicted by age. *Western Journal of Applied Forestry*, 5(4): 127-31.

Ranson, K. J. and Guoqing, S. 1994. Mapping biomass of a northern forest using multifrequency SAR data. *IEEE Transactions on Geoscience and Remote Sensing*, 32(2): 388-96.

Regelbrugge, J. C. and Conard, S. G. 1996. *Biomass and Fuel Characteristics of Chaparral in Southern California, 13th Conference on Fire and Forest Meteorology*, Oct. 27-31, 1996, Lorne, Australia.

Riggan, P. J., Goode, S., Jacks, P. M. and Lockwood, R. N. 1988. Interaction of fire and community devel-

opment in chaparral of southern california. *Ecological Monographs*, 58(3): 155-176.

Roberts, D. A. *et al*. 1998. Mapping chaparral in the Santa Monica Mountains using multiple endmember spectral mixture models. *Remote Sensing of Environment*, 65(3): 267-279.

Roberts, D. A., Green, R. O. and Adams, J. B. 1997. Temporal and spatial patterns in vegetation and atmospheric properties from AVIRIS. *Remote Sensing of Environment*, 62(3): 223-240.

Schlesinger, W. H. and Gill, D. S. 1980. Biomass, production, and changes in the availability of light, water, and nutrients during the development of pure stands of the chaparral shrub *Ceanothus megacarpus*, after fire. *Ecology*, 61(4): 781-9.

Specht, R. L. 1969. A comparison of the sclerophyllous vegetation characterisitc of mediterranean type climates in France, California, and Southern Australia. *Australian Journal of Botany*, 17: 293-308.

van Zyl, J. J., B. D. Chapman, P. Dubois, and J. C. Shi. (1993). "The effect of topography on SAR calibration." *IEEE Transactions on Geoscience and Remote Sensing* 31: 1036-43.

Wang, Y., Davis, F. W., Melack, J. M., Kasischke, E. S. and Christensen, N. L., Jr. (1995). The effects of changes in forest biomass on radar backscatter from tree canopies. *International Journal of Remote Sensing*: 503-513.

Wang, Y., Kasischke, E. S., Melack, J. M., Davis, F. W. and Christensen, N. L., Jr. (1994). The effects of changes in loblolly pine biomass and soil moisture on ERS-1 SAR backscatter. *Remote Sensing of Environment*: 25-31.